# Efficient removal of cadmium (II) ions from aqueous solution by $CoFe_2O_4$/chitosan and $NiFe_2O_4$/chitosan composites as adsorbents

Ashraf Homayonfard, Mahsasadat Miralinaghi, Reza Haji Seyed Mohammad Shirazi and Elham Moniri

## ABSTRACT

Magnetically recoverable chitosan based spinel cobalt and nickel ferrite (CS/$CoFe_2O_4$ and CS/$NiFe_2O_4$, respectively) composites were successfully prepared in one step. A series of batch adsorption experiments indicated that the removal of toxic Cd(II) ions by the as-obtained composites as adsorbents was pH-dependent, rapid, proficient, better fitted to pseudo-second-order kinetics model and Langmuir monolayer adsorption isotherm model. Compared to the naked particles, magnetic bio-polymer composites exhibited promoted adsorption capacity. Competitive adsorption studies in binary solutions illustrated preferable selectivity of adsorbents toward Cd(II) ions in the presence of co-existing cations. More importantly, CS/$CoFe_2O_4$ and CS/$NiFe_2O_4$ had a satisfactory practical application in the removal of Cd(II) from real groundwater spiked with cadmium. The exhausted adsorbents could be regenerated efficiently by 0.5 M $HNO_3$. The results from this study support that CS/$CoFe_2O_4$ and CS/$NiFe_2O_4$ prove excellent adsorption behavior for the removal of Cd(II) ions from aqueous media.

**Key words** | adsorption, cadmium, heavy metal, magnetic chitosan

**Ashraf Homayonfard**
**Reza Haji Seyed Mohammad Shirazi**
Faculty of Natural Resources and Environment,
Tehran Science and Research Branch,
Islamic Azad University,
Tehran,
Iran

**Mahsasadat Miralinaghi** (corresponding author)
**Elham Moniri**
Department of Chemistry, Faculty of Science,
Varamin-Pishva Branch ,
Islamic Azad University,
Varamin,
Iran
E-mail: *msmiralinaghi@gmail.com*;
*m_miralinaghi@iauvaramin.ac.ir*

## INTRODUCTION

Water is one of the most crucial resources for human beings and is considered as a significant economic, social, political, and environmental element, all over the world. In recent years, water pollution has become a great number of serious environmental and health problems; in particular, the entry of a myriad of various pollutants into water systems as a consequence of the rapid rise of urbanization and industrialization has attracted considerable global awareness (Reddy & Lee 2013). Pollutants being the major concerns include potentially toxic elements, dyes, phenolic compounds, pesticides, and herbicides to emerging micro-pollutants such as endocrine disrupting chemicals, pharmaceuticals and personal care products, and nitrosamines (Chowdhury & Balasubramanian 2014).

Cadmium is one of the non-biodegradable and extremely toxic heavy metals that often enter into the aquatic environment by various sources. The main source of cadmium in wastewaters is discharging of the waste stream through metallurgical alloying, ceramics, metal plating, and sewage sludge. Cadmium and its compounds are relatively water soluble over an extended range of pH compared to other metals; therefore, it has high mobility and easy biological accumulation (Tiwari & Mok 2017). Once in the human system, cadmium is known to build up primarily in the kidneys, throughout life, without being excreted, eventually damaging the renal, digestive and even the nervous systems. It also causes bone degradation, cancer, hypertension, and Itai-itai disease (Tshwenya & Arotiba 2017). The maximum allowable concentration of cadmium in drinking water is 0.003 mg $L^{-1}$ as legislated by the World Health Organization (WHO). Hence, in order to provide a safe and clean water supply to the public, there is a crucial need to take some measures to deal with the wastewaters containing a high amount of cadmium prior to their disposal.

Researchers in materials, analytical, and environmental sciences chemistry have tried to develop or improve remediation technologies for reducing or even eliminating

doi: 10.2166/wst.2018.510

cadmium and other heavy/hazardous metals (Carolin *et al.* 2017). Recently, adsorption has been the preferred technology for removal of different contaminants (both inorganic and organic), with cadmium included in a simple, economical, environment-friendly, and highly efficient way (Tshwenya & Arotiba 2017; Yadaei *et al.* 2018). As the adsorbent is the key to the adsorption process, many researches have been focused to develop high-performance adsorbents. Owing to their efficient adsorption performance, low cost, environment friendly nature, as well as readily available raw materials, chitosan and its derivatives have been tested widely and found to be effective for cadmium remediation through adsorption technology (Karthik & Meenakshi 2015; Olivera *et al.* 2016; Xu *et al.* 2016; Tiwari & Mok 2017). Due to the unique polycationic structure of chitosan, protonation of amine groups in acidic media ensures its ability to adsorb metal anions by ion exchange. The chelating properties of chitosan and its composites for metal ions have been discussed (Nguyen & Huynh 2014). Chelation can be attributed to the abundance of functional groups (such as acetamido, primary amino, and/or hydroxyl groups), which provides the coordinating capability with different metal ions. The chitosan selectivity is a remarkably eligible feature, as alkali metal and alkali earth metal ions (which are plentiful but not toxic) are not chelated, but transition metals and post-transition metal ions (usually scarce in quantities and extremely toxic) are removed. The sequestration of chitosan-based adsorbents from the aqueous solution after the adsorption process with conventional separation methods such as filtration and sedimentation can be challenging, because they may block the filters or be lost. In addition, adsorbent materials when released in the environment can cause secondary pollution due to their sludge production (Reddy & Lee 2013; Kefeni *et al.* 2017).

Recently, in order to overcome the mentioned problems and to facilitate the separation and recycling of absorbent materials, the process of magnetic separation has been proposed as an alternative scheme in water and wastewater treatment. The fundamental advantage of this technology is the rapid separation from wastewater using minimal energy consumption and production of no contaminant (Dai *et al.* 2017).

In this study, the possibility of using magnetic cobalt and nickel ferrite particles covered with chitosan (CS/$CoFe_2O_4$ and CS/$NiFe_2O_4$, respectively) as adsorbents for the removal of cadmium (II) from aqueous solutions is investigated.

## EXPERIMENTAL SECTION

### Preparation of adsorbents

In a typical procedure, 2.7 g $FeCl_3.6H_2O$ and 1.19 g $CoCl_2.6H_2O$ ($NiCl_2.6H_2O$) were dissolved in 40 mL double-distilled water (DDW) followed by intensive sonicating for 30 min to form a homogeneous solution, which was denoted as solution A. Chitosan solution was prepared by dissolving 0.8 g chitosan into 50 mL acetic acid (2% v/v). To prepare CS/$CoFe_2O_4$ (CS/$NiFe_2O_4$) composite, the chitosan solution was slowly added to the solution A. The temperature of the mixture solution was raised to 80 °C under simultaneous vigorous stirring. Subsequently, the pH of the solution was increased to 10.5 by adding droplets of 2 M NaOH. Afterwards, 0.5 mL 25 wt.% glutaraldehyde as a cross-linking agent was added into the mixture. The resulting brownish red suspension was sealed in a Teflon-lined stainless steel autoclave and maintained at 200 °C for 4 h in a furnace. The reaction product was collected with the help of a magnet, rinsed with DDW and ethanol to remove residual chitosan and inorganic ions, and finally was dried at 60 °C for 10 h in a hot air oven. Naked $CoFe_2O_4$ ($NiFe_2O_4$) particles were prepared in the same procedure without the addition of chitosan solution. Detailed information about the characterization techniques can be found in the supplementary information (available with the online version of this paper).

### Batch adsorption procedure

A stock solution (500 mg $L^{-1}$ and 50 mL) of Cd(II) was prepared by dissolving an appropriate amount (0.069 g) of $Cd(NO_3)_2.6H_2O$ in deionized water.

The effect of solution pH on Cd(II) adsorption onto the as-prepared CS/$CoFe_2O_4$ and CS/$NiFe_2O_4$ as adsorbents was investigated by adjusting the pH of the Cd(II) ion solution from 3 to 9 using 10 mL of 0.1 M acetic acid–acetate buffer (pH 3–6.5) or 0.01M phosphate buffer (pH 6.5–9). 0.05 g of adsorbent was added to 25 mL Cd(II) solution with an initial concentration of 10 mg $L^{-1}$ and shaken for 120 min.

The adsorption kinetics were studied with 25 mL Cd(II) solution of three different initial concentrations (10, 20, 40 mg $L^{-1}$) at pH 7.0 with an adsorbent dose of 0.05 g. The mixture was shaken for a fixed period of time, varying from 5 to 90 min.

To explore the adsorption isotherms, 0.05 g of adsorbent was mixed with 10 mL of Cd(II) solution of different initial

concentrations in the range of 5–120 mg $g^{-1}$ at pH 7.0. The mixtures were shaken for 60 min.

For searching the effect of coexisting metal ions with Mn(II), Pb(II), Zn(II) and Cu(II) cations, 25 mL binary solution containing 20 mg $L^{-1}$ of Cd(II), and each of the above ions with the same concentration and 0.05 g of adsorbent were agitated on a shaker together and kept for 60 min with adjusting to pH 6.0.

After adsorption, the adsorbent was separated by using an external magnetic field and the concentrations of residual Cd(II) ions in the supernatant were determined by atomic absorption spectroscopy (AAS).

All experiments were conducted at 298 K and 200 rpm in duplicate and the relative errors were less than 5%. The adsorption amount of Cd(II) ions at time $t$ ($q_t$, mg $g^{-1}$), and the removal efficiency (R(%)) were calculated by Equations (1) and (2), respectively.

$$q_t = \frac{(C_0 - C_t)\,V}{M} \tag{1}$$

$$\mathrm{R}(\%) = \frac{(C_0 - C_t)}{C_0} \times 100 \tag{2}$$

where $C_0$ and $C_t$ (mg $L^{-1}$) represent the initial and time $t$ concentration of the ion solution, respectively, $V$ (L) is the volume of ion solution and $M$ (g) is the mass of dried adsorbent.

### Preparation of real groundwater spiked with Cd(II) for adsorption testing

Real groundwater was collected from Kukeneh village in Blukat Rural District, Rahmatabad and Blukat District, Rudbar County, Gilan Province, Iran. The initial concentration of Cd(II) ions in the water samples which has been determined by the spectrophotometric method were less than the detection limit. 10 mL of 100 mg $L^{-1}$ of Cd(II) solution was taken into the 100 mL standard flask and diluted with filtered real groundwater to aim at the final concentration of 10 mg $L^{-1}$, with adjusting to pH 7.0. Then, 0.05 g of adsorbent was added to the 25 mL spiked samples and shaken for 60 min.

### Regeneration and reusability testing

To explore the desorption and reusability performance of the adsorbent, 0.05 g of as-prepared CS/$CoFe_2O_4$ (or CS/$NiFe_2O_4$) was applied to treat 25 mL water contaminated with Cd(II) at 10 mg $L^{-1}$. After adsorption equilibrium had been achieved, the adsorbent separated and the supernatant solution was analyzed by AAS. Then, the exhausted adsorbent was thoroughly eluted in 10 mL of 0.5 M $HNO_3$ as a desorbing agent as well as 10 mL deionized water and used for the next adsorption-desorption studies.

## RESULTS AND DISCUSSION

### Characterization of samples

Figure S1(a)–S1(c) (available with the online version of this paper) exhibit Fourier transform infrared (FTIR) spectra of the chitosan, CS/$CoFe_2O_4$ and CS/$NiFe_2O_4$ recorded in the range of 400–4,000 $cm^{-1}$. For chitosan in Figure S1(a), the bands at around 1,164–907 $cm^{-1}$ can be assigned to the glycosidic bands, C – O and C – O – C stretching from the polysaccharide skeleton. The bands located at 1,426 and 1,339 $cm^{-1}$ are corresponding to the vibrations of OH and CH in the ring. The peaks centered at 2,873, 1,660, and 1,608 $cm^{-1}$ are related to the –CH and $-CH_2$, amide I band and C=O stretch, $NH_2$ bending. The strong and broad peak appeared at around 3,423 $cm^{-1}$ is attributed to the stretching vibration of the N – H group bonded with O – H group (Fan *et al.* 2017). Compared with chitosan, the spectra of CS/$CoFe_2O_4$ and CS/$NiFe_2O_4$ in Figure S1(b) and S1(c) have all the predominant characteristic peaks of chitosan, which reflected the existence of chitosan in CS/$CoFe_2O_4$ and CS/$NiFe_2O_4$ composites. The decreasing intensities at 1,608 and 3,423 $cm^{-1}$ have fewer amine groups than chitosan, which may be due to the chelation between chitosan and metal ions (M = Co, Ni, Fe). The distinctive peak observed at around 600 $cm^{-1}$ is associated with metal-oxygen (M – O) stretching vibration.

The X-ray diffraction (XRD) patterns of CS/$CoFe_2O_4$ and CS/$NiFe_2O_4$ are shown in Figure S2(a) and S2(b), respectively (available online). The seven characteristic diffraction peaks of CS/$CoFe_2O_4$ (CS/$NiFe_2O_4$) observed at 18.3° (17.0°), 30.2° (27.0°), 35.5° (35.5°), 40.2° (40.0°), 43.3° (43.4°), 57.0° (56.4°), and 62.6° (64.7°) can be indexed to the (111), (220), (311), (400), (422), (511) and (440) planes of the inverse spinel $CoFe_2O_4$ ($NiFe_2O_4$) in accordance with the standard JCPDS card No. 22-1086 (86-2267) (Santhosh *et al.* 2015), indicating the stability of the crystalline phase of $CoFe_2O_4$ ($NiFe_2O_4$) particles during coating with chitosan. It is noted that a weak peak at 21° corresponded to the amorphous structure of chitosan in the as-prepared composites (Xiao *et al.* 2013). The average crystallite size, which is calculated by the Scherrer formula (Langford & Wilson 1978), yielded an approximate

value of 57 and 66 nm for $CoFe_2O_4$ and $NiFe_2O_4$ particles, in agreement with the FE-SEM observations.

The surface morphology of as-prepared composites was analyzed by field emission scanning electron microscopy (FE-SEM) captured at 50,000× magnification. As depicted in Figure S3(a) (available online), chitosan exhibits a relatively fiber-like porous structure with some holes and crevasses and no particles are observed on top. However, in Figure S3(b) and S3(c) for CS/$CoFe_2O_4$ and CS/$NiFe_2O_4$, respectively, $CoFe_2O_4$ and $NiFe_2O_4$ particles appear as bright dots with the regular shapes consisting of a number of clusters of various sizes, which are made of tiny particles, usually less than 70 nm. This may be ascribed to their magnetic property, which leads to a mild aggregation. In spite of the fact that clustering of magnetic particles may result in reducing adsorption efficiency, the combination of adsorption and magnetic properties into one composite allows obtaining of a magnetic adsorbent potentially, which can be removed from the medium by a magnetic separation method using an external magnetic field and without the use of filtration or centrifugation.

The quantitative elemental composition of chitosan and two composites (before and after adsorption of Cd(II) ions) was analyzed by energy-dispersive X-ray analysis spectrum (EDX). The EDX profile of chitosan in Figure 1(a) is dominated by carbon (C), oxygen (O), and nitrogen (N), indicating no other elemental impurities. The gold (Au) peak in the EDX profile is attributed to the gold tape used for the sample loading. The EDX spectra in Figure 1(b) and 1(c) confirm the formation of CS/$CoFe_2O_4$ and CS/$NiFe_2O_4$, respectively, where apart from chitosan, the contribution of $CoFe_2O_4$ and $NiFe_2O_4$ particles is clearly observed. In

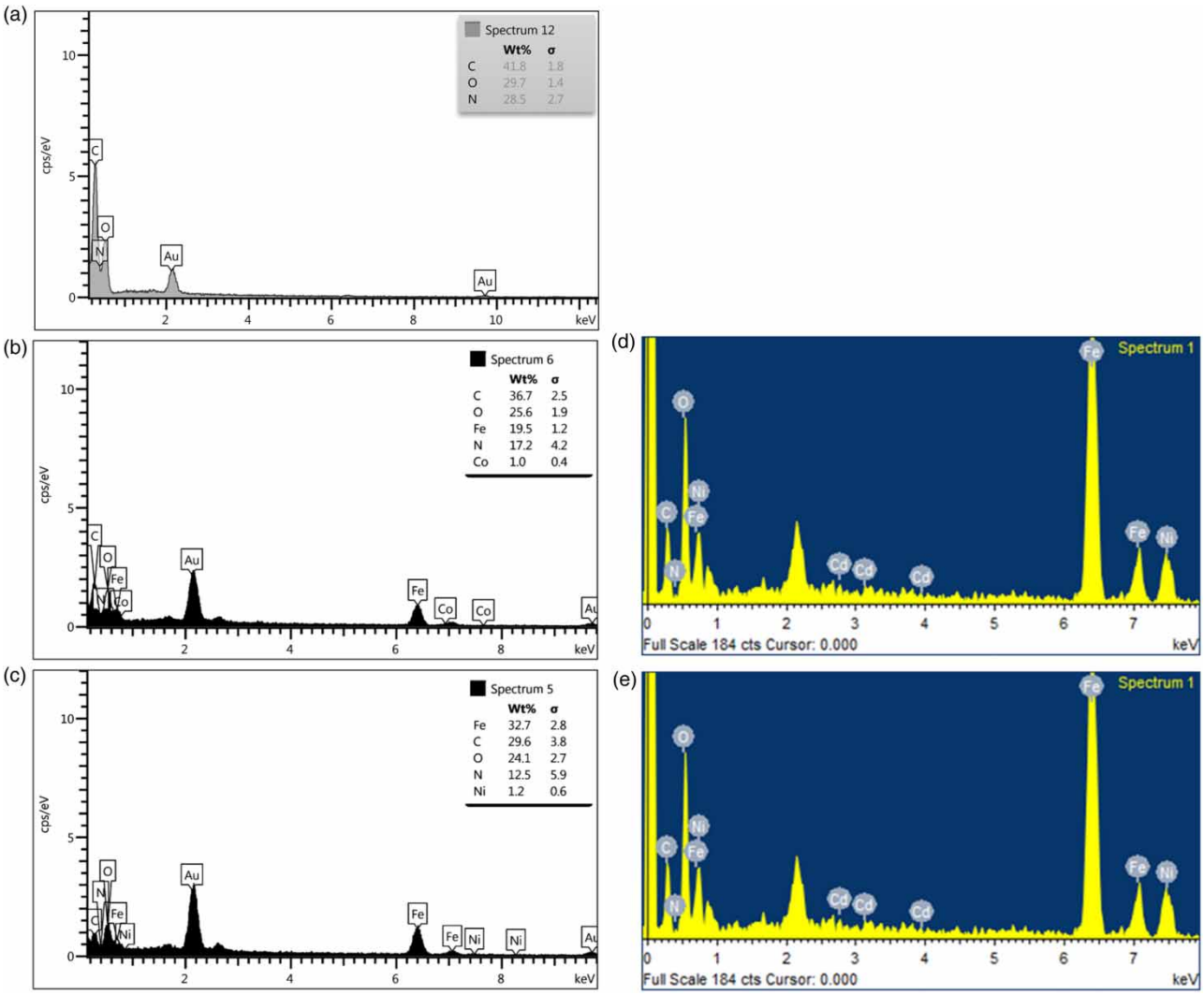


**Figure 1** | The EDX spectra of (a) chitosan, (b) CS/$CoFe_2O_4$, and (c) CS/$NiFe_2O_4$; the EDX spectra of (d) CS/$CoFe_2O_4$ and (e) CS/$NiFe_2O_4$ after Cd(II) ions adsorption.

addition to C, O, and N, the presence of Fe, and Co (or Ni) was supposed to arise from $CoFe_2O_4$ (or $NiFe_2O_4$). Also, after adsorption, the appearance of cadmium peaks along with the above-mentioned elements peaks, as shown in Figure 1(d) and 1(e), verifies that Cd(II) ions were successfully taken up onto the surface of CS/$CoFe_2O_4$ and CS/$NiFe_2O_4$.

VSM analyses were used to measure the magnetic properties of as-prepared composites at room temperature. Figure 2(a) and 2(b) show the hysteresis loops CS/$CoFe_2O_4$ and CS/$NiFe_2O_4$. The insets are magnified views of hysteresis loops at low applied fields. The saturation magnetization ($M_s$) remnant magnetization ($M_r$) and coercive force ($H_e$) of composites obtained from hysteresis loops are listed in Table S1 (available online), implying their ferromagnetic nature. The $M_s$ Values of CS/$CoFe_2O_4$ (CS/$NiFe_2O_4$) reaches 26.4 and 19.8 emu $g^{-1}$, respectively, suggesting these materials have a rapid response to an external magnetic field and can be separated from aqueous dispersion within a few seconds.

## Adsorption studies

### Effect of solution pH

The solution pH is a key operational parameter in the adsorption process because it can be an influence on the solution chemistry of metal ions as well as the state of functional groups on the surface of the adsorbent (Karaer & Kaya 2017). The effects of pH on the Cd(II) removal efficiency by CS/$CoFe_2O_4$ and CS/$NiFe_2O_4$ magnetic composite were monitored over the range of pH values from 3–9 by keeping the concentration of Cd(II) (10 mg $L^{-1}$) and adsorbent (0.05 g) constant. As shown in Figure S4 (available online), at lower pH the removal of Cd(II) was not significant. With the increase in pH from 4 to 6, the removal efficiency drastically raised from 60 to 98.5% for CS/$CoFe_2O_4$ and from 50 to 97% for CS/$NiFe_2O_4$. Beyond this pH range, nearly 100% removal was obtained, which is probably owing to the simultaneous effect of adsorption and precipitation of Cd(II).

At acidic pH, the primary amine groups of chitosan coating the surface of adsorbents are easily protonized to form $-NH_3^+$ cations, which would result in electrostatic repulsion with the positively charged Cd(II) ions. As more $-NH_2$ groups are converted to $-NH_3^+$, there are fewer $-NH_2$ binding sites available on the surface for complexing with Cd(II) ions, leading to the considerable reduction of adsorption at lower pH (Chen *et al.* 2015). Conversely, a gradual increase in pH causes a decrease of $H_3O^+$ and weakening of the protonated ability of the primary amine, thereby the Cd(II) removal efficiency is promoted. According to the species distribution, the cadmium predominantly exists as $Cd^{2+}$ soluble cation up to pH 8.8 (Tiwari & Mok 2017) and beyond this pH, it begins to precipitate as $Cd(OH)_2$. It is also observed that a slight amount of $Cd(OH)^+$ species is formed between pH 8 to 10. An optimum pH of 7.0 was selected for further adsorption experiments.

### Effect of contact time and initial Cd(II) ion concentration

The contact time required to reach adsorption balance is one of the most important parameters in the design of an

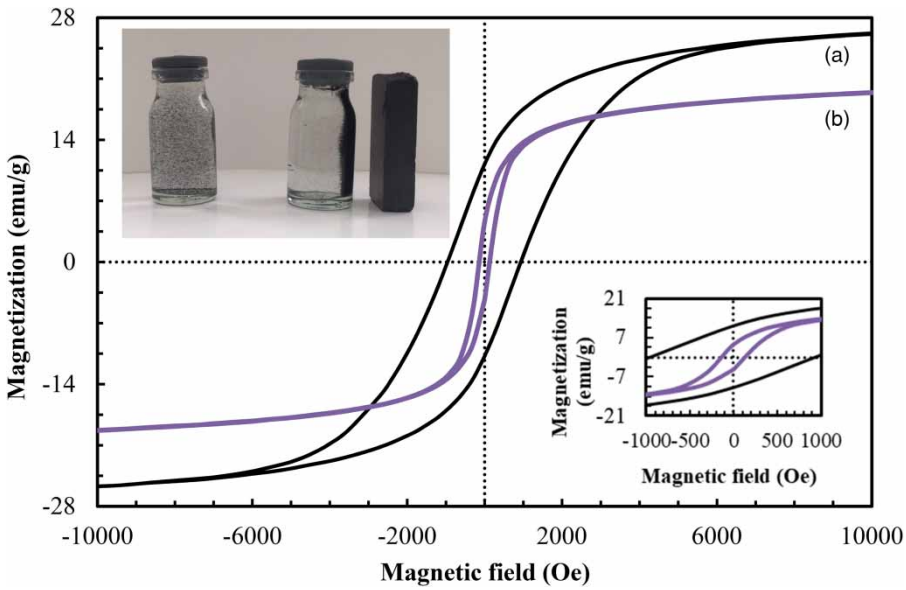


**Figure 2** | Magnetization curves measured at room temperature for (a) CS/CoF $e_2O_4$ and (b) CS/$NiFe_2O_4$. Insets are magnified views of the hysteresis loops at the low applied field.

economical adsorption system. Figure 3(a) and 3(b) present removal efficiencies of Cd(II) ions with the initial concentration of 10, 20, and 40 mg $L^{-1}$ at pH of 7.0 onto CS/$CoFe_2O_4$ and CS/$NiFe_2O_4$, respectively as a function of time. It is clearly observed that the removal efficiency raised sharply at the initial stage and subsequently increased at a slow speed; afterwards, it no longer changed even with the contact time prolonged. The initial extremely rapid adsorption rate is mainly attributed to the abundant vacant active sites on the adsorbent surfaces, and the quick diffusion of Cd(II) ions from the solution to the adsorbent pores. As the adsorption process proceeded, gradual occupancy of the surface sites slowed down the adsorption rate and the adsorption tended to equilibrium (Li *et al.* 2017).

The reduction of Cd(II) removal efficiency with an increase of initial ion concentration may be due to the fact that at the higher initial Cd(II) concentration, the total existing adsorptive sites are confined as a result of a fixed amount of adsorbent. However, the maximum removal efficiencies of 95% and 92% were observed within 90 min at initial Cd(II) concentration of 40 mg $L^{-1}$ with CS/$CoFe_2O_4$ and CS/$NiFe_2O_4$, respectively. Moreover, in the solution with lower ion concentration, equilibrium was reached faster because of the stronger adsorption driving forces as well as weaker repulsive forces between the Cd(II) ions on the solid and in the bulk phases as compared to the ion solutions of higher concentration. In the solution of 10 and 20 mg $L^{-1}$ Cd(II) concentration, equilibrium was achieved within about 30 min, whereas in the solution of 40 mg $L^{-1}$ Cd(II) concentration the adsorption reached the equilibrium at the far longer time of 90 min with both CS/$CoFe_2O_4$ and CS/$NiFe_2O_4$.

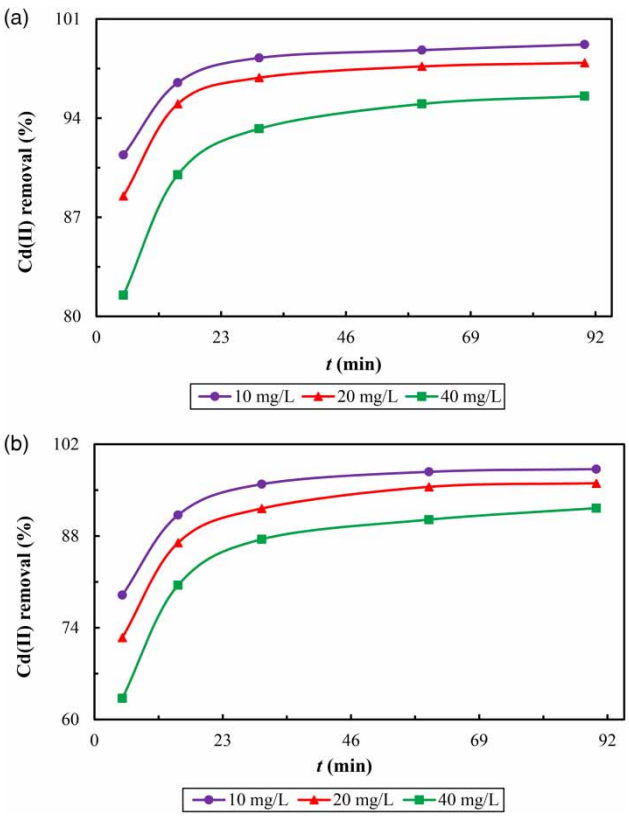


**Figure 3** | Effect of contact time and initial ion concentration on Cd(II) removal efficiency with (a) CS/$CoFe_2O_4$ and (b) CS/$NiFe_2O_4$. Experimental conditions: pH 7.0, 0.05 g of adsorbent, 25 mL of Cd(II) solution.

## Effect of coexisting cations

In most cases, water contaminated with various toxic metal ions and the sample matrix may interfere with the removal efficiency for ions of Cd(II) in media (Moradi *et al.* 2017). In order to probe the effects of coexisting cationic ions on the degree of Cd(II) selectivity, adsorption experiments were carried out in the binary solutions containing metal ions such as Mn(II), Pb(II), Zn(II), and Cu(II) with equal concentration of Cd(II) (20 mg $L^{-1}$). According to the Cu(II) distribution as a function of pH (Fan *et al.* 2017), the copper ion mainly exists in the form of $Cu^{2+}$ when the solution pH is less than 6.0. Consequently, a pH of 6.0 was selected for the adsorption experiments. The obtained results are shown in Figure 4. It is clearly observed that Mn(II) and Pb(II) ions had no obvious effects on the adsorption performance for both adsorbents. However, the presence of Zn(II) ions resulted in a slight decrease in Cd(II) adsorption. The remove efficiencies of Cd(II) in binary Cd(II) and Cu(II) solutions decreased from 91% to 65% CS/$CoFe_2O_4$ and from 86% to 55% by CS/$NiFe_2O_4$ compared to single Cd(II) solution. These results illustrated that Cu(II) ions have significant suppressive impact on Cd(II) adsorption, whereas Mn(II), Pb(II), and Zn(II) ions exhibit no apparent or little influence on the uptake of Cd(II). This observation can be explained by changes of the competitive adsorption ability from one metal ion to another, which may be related to some factors, for instance, molecular mass, ion charges, hydrated ionic radius and hydration energy of ionic metal (Xiang *et al.* 2017).

## Application of adsorbents for real groundwater spiked with Cd(II)

In order to assess the applicability of CS/$CoFe_2O_4$ and CS/$NiFe_2O_4$ for the removal of Cd(II) from the real groundwater, 5 mg $L^{-1}$ of Cd(II) was spiked after filtration

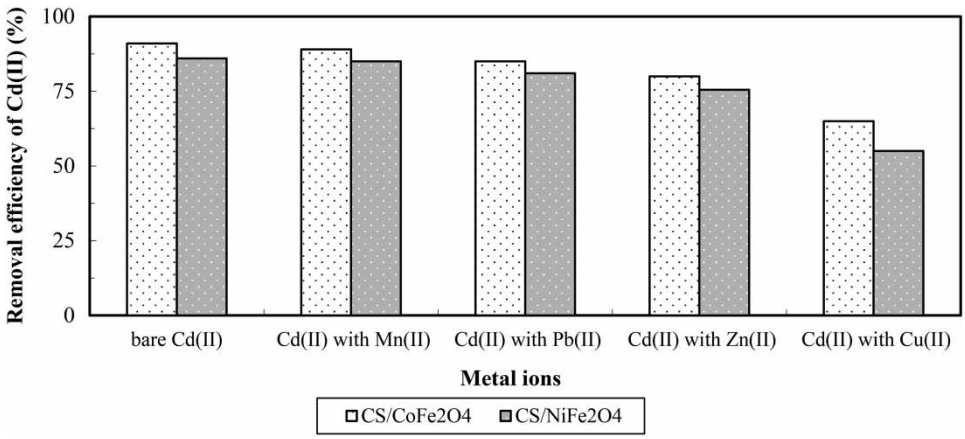


**Figure 4** | Effect of coexisting cations on Cd(II) removal efficiency. Experimental conditions: pH 6.0, 0.05 g of adsorbent, 25 mL of 20.0 mg $L^{-1}$ of Cd(II) and coexisting cation in binary solution, and contact time of 60 min.

of water through a membrane. The removal results are shown in Table S2 (available online). Almost 99.2% (93.5%) of Cd(II) ions were adsorbed from spiked real samples by CS/$CoFe_2O_4$ (CS/$NiFe_2O_4$) composite. This apparently suggests that prepared magnetic chitosan composites can be utilized for the effective treatment of real groundwater containing cadmium.

## Regeneration and reusability of adsorbents

An ideal adsorbent should have high adsorption capacity as well as excellent regeneration ability, which make the adsorption process more economical and applicable. To assess the regeneration performance of spent adsorbents, the CS/$CoFe_2O_4$ and CS/$NiFe_2O_4$ after uptake of Cd(II) ions were eluted with 0.5 mol $L^{-1}$ $HNO_3$ solution as the desorbing agent and reused for metal adsorption. As shown in Figure S5 (available online), after seven consecutive adsorption/desorption cycles, the desorbing efficiencies were above 70% for both adsorbents. Therefore, these composites possess good properties for repeated use. The slight drop in removal efficiencies studies may be attributed to the loss of adsorbents and decrease of active sites after each desorption steps (Guo *et al.* 2016).

## Cd(II) adsorption kinetics

In order to further understand the mechanism of the ion adsorption process and potential rate controlling step, the experimental data were analyzed according to different well-known kinetics models such as pseudo-first-order (PFO) (Lagergren 1898), pseudo-second-order (PSO) (Ho & McKay 1999), Elovich (Chien & Clayton 1980), and intra-particle diffusion (Weber & Morris 1963) at three initial Cd(II) concentrations: 10, 20, 40 mg $L^{-1}$ (details provided in the supplementary material, available online).

The value of all kinetic parameters and the correlation coefficients ($R^2$) calculated from the non-linear fitting of four models are summarized in Table 1. The $R^2$ values of the PSO kinetic curves exceeded 0.9999. Furthermore, the $q_{e,cal}$ values determined from PSO kinetic models agreed better with the experimental values, $q_{e,exp}$, for all concentrations studied (Table 1). Hence, the adsorption process of Cd(II) ions onto CS/$CoFe_2O_4$ and CS/$NiFe_2O_4$ followed the PSO model. That is the adsorption of Cd(II) onto magnetic ferrite chitosan composites, in part, from the chemical reaction between the amino or hydroxyl groups on chitosan and the metal ions.

The decrease of $k_2$ with the increase of initial Cd(II) concentration can be due to the longer time required to reach the equilibrium state. Additionally, from Table 1, the obtained $h$, initial rate, and $k_2$, PSO rate constant, values for Cd(II) adsorption onto CS/ $CoFe_2O_4$ were all much higher than those of CS/ $NiFe_2O_4$, suggesting that the rate of adsorption onto CS/ $CoFe_2O_4$ was faster than that of CS/ $NiFe_2O_4$.

Typically, various mechanisms control the adsorption kinetics; the most limiting were the diffusion mechanisms, including external diffusion, boundary layer diffusion and intra-particle diffusion (Hamza *et al.* 2013). Hence, the intra-particle diffusion model was also utilized to explain the rate-limiting step of the adsorption process (Deniz & Saygideger 2010). The correlation coefficients, $R^2$, for this model had relatively high values (>0.99), indicating the intra-particle diffusion played a key role in the adsorption process of Cd(II). But the non-zero values of the intercept, $C$, revealed that intra-particle diffusion was not the exclusive

**Table 1** | Non-linear kinetic parameters for the adsorption of Cd(II) with different initial concentration onto adsorbents[a]

| | | CS/$CoFe_2O_4$ | | | CS/$NiFe_2O_4$ | | |
|---|---|---|---|---|---|---|---|
| | | Initial Cd(II) concentration (mg $L^{-1}$) | | | Initial Cd(II) concentration (mg $L^{-1}$) | | |
| **Kinetics models** | **Parameters** | **10** | **20** | **40** | **10** | **20** | **40** |
| Pseudo-first order | $k_1$ ($min^{-1}$) | 0.5333 | 0.4886 | 0.4072 | 0.3412 | 0.2938 | 0.2379 |
| | $q_{e,cal}$ (mg $g^{-1}$) | 4.9101 | 9.6876 | 18.7082 | 4.8007 | 9.3139 | 17.7292 |
| | $R^2$ | 0.9998 | 0.9997 | 0.9995 | 0.9993 | 0.9989 | 0.9985 |
| | $q_{e,exp}$ (mg $g^{-1}$) | 4.9600 | 9.7900 | 19.1100 | 4.9100 | 9.6050 | 18.4500 |
| Pseudo-second order | $k_2$ (g $mg^{-1}$ $min^{-1}$) | 0.4441 | 0.1782 | 0.0564 | 0.1511 | 0.0576 | 0.0212 |
| | $q_{e,cal}$ (mg $g^{-1}$) | 4.9804 | 9.8592 | 19.2485 | 4.9896 | 9.7869 | 18.9002 |
| | $h$ (mg $g^{-1}$ $min^{-1}$) | 11.0175 | 17.3228 | 18.6974 | 3.7624 | 5.5189 | 7.5742 |
| | $R^2$ | 1.0000 | 1.0000 | 1.0000 | 1.0000 | 1.0000 | 1.0000 |
| | $q_{e,exp}$ (mg $g^{-1}$) | 4.9600 | 9.7900 | 19.1100 | 4.9100 | 9.6050 | 18.4500 |
| Simplified Elovich | $\alpha$ (mg $g^{-1}$ $min^{-1}$) | $4.4919 \times 10^{13}$ | $1.2211 \times 10^{11}$ | $5.6403 \times 10^{6}$ | 14,639.6 | 1681.33 | 322.886 |
| | $\beta$ (g $mg^{-1}$) | 7.5854 | 3.1453 | 1.03459 | 3.0208 | 1.2292 | 0.5046 |
| | $R^2$ | 0.9999 | 0.9998 | 0.9997 | 0.9994 | 0.9993 | 0.9989 |
| Intraparticle diffusion | $k_i$ (mg $g^{-1}min^{-1/2}$) | 0.0474 | 0.1134 | 0.3519 | 0.1192 | 0.2958 | 0.7224 |
| | $C$ (mg $g^{-1}$) | 4.5685 | 8.8641 | 16.1839 | 3.9338 | 7.1596 | 12.3964 |
| | $R^2$ | 0.9998 | 0.9996 | 0.9993 | 0.9985 | 0.9979 | 0.9967 |

[a]Experimental conditions: pH 7.0, 0.05 g of adsorbent, 25 mL of Cd(II) solution.

rate-limiting step for the whole process. Also from Table 1, the values of the intercept, $C$, increased with the initial Cd(II) concentration. This demonstrated that augmenting the initial ion concentration promoted the thickness and effect of the boundary layer diffusion.

### Cd(II) adsorption isotherms

To further investigate the nature of the interaction of Cd(II) metal ions with CS/$CoFe_2O_4$ and CS/$NiFe_2O_4$ and to compare the adsorption capacity of these two composites with naked $CoFe_2O_4$ and $NiFe_2O_4$ particles, the equilibrium adsorption data were analyzed by four well-known adsorption isotherm models, namely Langmuir (Langmuir 1918), Freundlich (Freundlich 1906), Dubinin-Radushkevich (DR) (Dubinin & Radushkevich 1947), and Temkin (Temkin & Pyzhev 1940) over the initial Cd(II) concentration range of 5–120 mg $L^{-1}$ (details of isotherm equations are provided in the supplementary material, available online).

Figure 5 displays the non-linear plots of fitting models. The value of isotherm parameters along with the correlation coefficients, $R^2$, obtained from the non-linear regression are listed in Table 2. It is obvious that the Langmuir model with higher values of $R^2$ ($R^2 > 0.999$) fitted the experimental equilibrium data better than the other models. Hence, the Cd(II) adsorption process obeyed the Langmuir isotherm. That is, all the adsorption sites are energetically identical, and thus have an equal affinity to Cd(II) ions and a monolayer adsorption process takes place on the homogeneous adsorbent surface. With respect to adsorption capacity, the $q_m$ reached 26.35 and 25.55 mg $g^{-1}$ for Cd(II) ion adsorption onto CS/$CoFe_2O_4$ and CS/$NiFe_2O_4$ composites, which were relatively higher than the $q_m$ of naked $CoFe_2O_4$ and $NiFe_2O_4$ particles (23.27 and 20.55 mg $g^{-1}$, respectively).

The essential characteristics of the Langmuir isotherm can be expressed in terms of a dimensionless constant separation factor, $R_L$, defined by Equation (3).

$$R_L = \frac{1}{1 + K_L C_0} \tag{3}$$

where $K_L$ (L $mg^{-1}$) is the Langmuir constant and $C_0$ (mg $L^{-1}$) is the highest initial Cd(II) concentration (Panahi *et al.* 2012). The $R_L$ values given in Table 2 were in the range of 0–1, indicating that the Cd(II) adsorption processes are favorable under the conditions used in this study. For the Freundlich isotherm, the values of $n$, related to the adsorption intensity, were greater than 1, which confirmed that the Cd(II) ions are favorably adsorbed onto the surface of all four adsorbents.

## CONCLUSION

In this study, magnetic CS/$CoFe_2O_4$ and CS/$NiFe_2O_4$ composites were easily prepared, structurally characterized, and

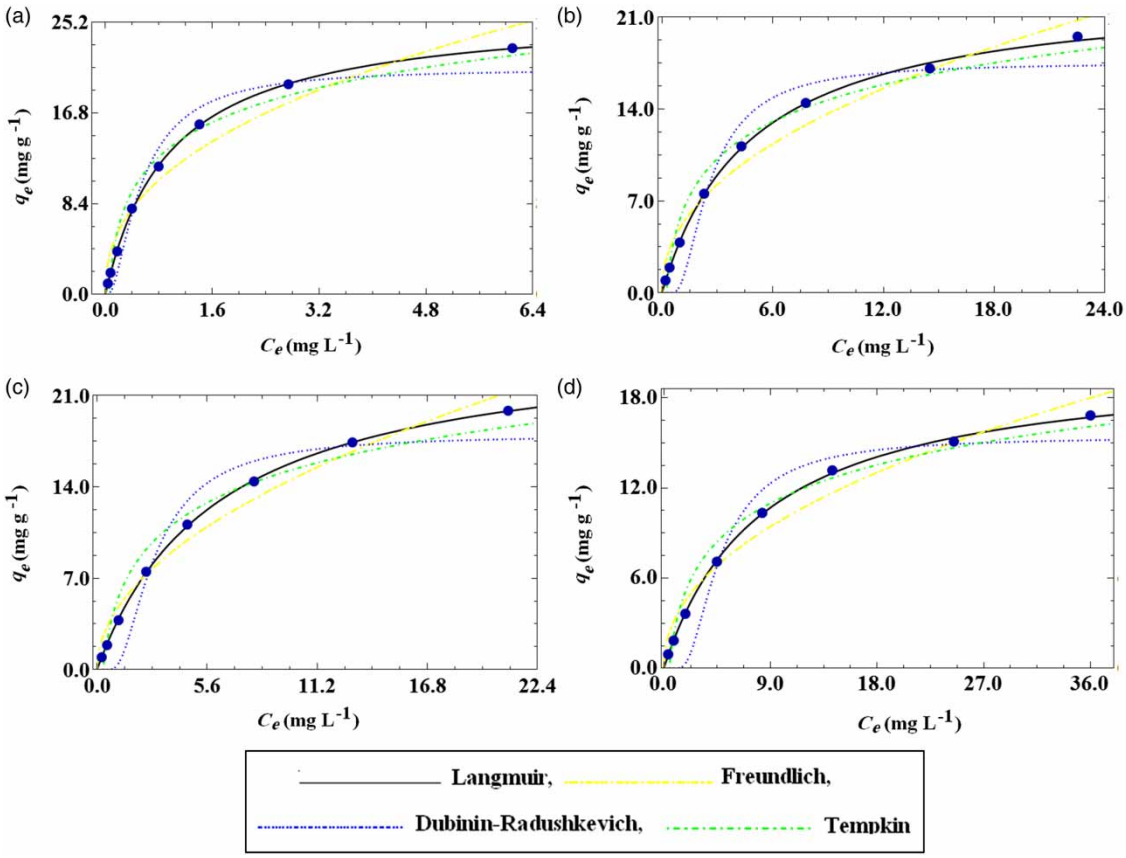


**Figure 5** | Non-linear plots of isotherm models for the adsorption of Cd(II) onto (a) CS/$CoFe_2O_4$, (b) naked $CoFe_2O_4$, (c) CS/$NiFe_2O_4$, and (d) naked $NiFe_2O_4$. The dark blue circles show experimental data. Experimental conditions: pH 7.0, 0.05 g of adsorbent, 10 mL of Cd(II) solution, contact time of 60 min. The full colour version of this figure is available in the online version of this paper, at http://dx.doi.org/10.2166/wst.2018.510.

**Table 2** | Non-linear isothermal parameters for the adsorption of Cd(II) onto adsorbents[a]

| | | Adsorbent | | | |
|---|---|---|---|---|---|
| **Isotherm models** | **Parameters** | **CS/$CoFe_2O_4$** | **$CoFe_2O_4$** | **CS/$NiFe_2O_4$** | **$NiFe_2O_4$** |
| Langmuir | $q_m$ (mg g$^{-1}$) | 26.347 | 23.2861 | 25.5534 | 20.5513 |
| | $K_L$ (L mg$^{-1}$) | 1.0393 | 0.2089 | 0.1643 | 0.1205 |
| | $R_L$ | 0.0079 | 0.0384 | 0.0483 | 0.0646 |
| | $R^2$ | 0.9999 | 0.9997 | 0.9999 | 0.9998 |
| Freundlich | $K_F$ $\left(\text{mg}^{1-\frac{1}{n}}\text{L}^{\frac{1}{n}}\text{g}^{-1}\right)$ | 11.6156 | 4.996 | 4.5989 | 3.3936 |
| | $n$ | 2.3772 | 2.1869 | 1.9876 | 2.1482 |
| | $R^2$ | 0.9819 | 0.9896 | 0.9910 | 0.9896 |
| Dubinin-Radushkevich | $q_s$ (mg g$^{-1}$) | 20.8653 | 17.5123 | 17.9643 | 15.4014 |
| | $k_{ad}$ (mol$^2$ kJ$^{-2}$) | 0.1064 | 1.1293 | 1.3839 | 3.2797 |
| | $R^2$ | 0.9863 | 0.9760 | 0.9758 | 0.9753 |
| Temkin | $A_T$ (L mg$^{-1}$) | 19.576 | 4.0799 | 3.2282 | 2.1949 |
| | $b_T$ (J g mol$^{-1}$ mg$^{-1}$) | 535.9310 | 608.199 | 561.708 | 673.171 |
| | $R^2$ | 0.9907 | 0.9895 | 0.9870 | 0.9909 |

[a]Experimental conditions: pH 7.0, 0.05 g of adsorbent, 10 mL of Cd(II) solution, contact time of 60 min.

systematically used as an environmentally friendly adsorbent for the efficient and rapid removal of Cd(II) ions from aqueous media. The adsorption kinetic data fitted well with the pseudo-second-order kinetic model. The adsorption was also best described by the Langmuir isotherm, with a maximum monolayer adsorption capacity of

26.35 and 25.55 mg $g^{-1}$ for CS/$CoFe_2O_4$ and CS/ $NiFe_2O_4$, respectively, at 298 k and pH 7.0. Prepared composites illustrated high selectivity toward Cd(II) in the presence of coexisting cationic ions in binary solutions. After seven successive adsorption-desorption cycles, the adsorption capacity of the adsorbents was considerably retained.

## REFERENCES


Carolin, C. F., Kumar, P. S., Saravanan, A., Joshiba, G. J. & Naushad, M. 2017 Efficient techniques for the removal of toxic heavy metals from aquatic environment: a review. *Journal of Environmental Chemical Engineering* **5** (3), 2782–2799.

Chen, J. H., Xing, H. T., Sun, X., Su, Z. B., Huang, Y. H., Weng, W., Hu, S. R., Guo, H. X., Wu, W. B. & He, Y. S. 2015 Highly effective removal of Cu(II) by triethylenetetramine-magnetic reduced graphene oxide composite. *Applied Surface Science* **356**, 355–363.

Chien, S. H. & Clayton, W. R. 1980 Application of Elovich equation to the kinetics of phosphate release and sorption in soils. *Soil Science Society of America Journal* **44** (2), 265.

Chowdhury, S. & Balasubramanian, R. 2014 Recent advances in the use of graphene-family nanoadsorbents for removal of toxic pollutants from wastewater. *Advances in Colloid and Interface Science* **204**, 35–56.

Dai, J., Zhao, H., Ye, Y., Wang, L., Cao, S., Su, X., Hu, X. & Li, L. 2017 Improving the selectivity of magnetic graphene oxide through amino modification. *Water Science and Technology* **76** (11), 2959–2967.

Deniz, F. & Saygideger, S. D. 2010 Equilibrium, kinetic and thermodynamic studies of Acid Orange 52 dye biosorption by *Paulownia tomentosa* Steud. leaf powder as a low-cost natural biosorbent. *Bioresource Technology* **101** (14), 5137–5143.

Dubinin, M. M. & Radushkevich, L. V. 1947 The equation of the characteristic curve of the activated charcoal. *Proc. Acad. Sci. USSR Phys. Chem. Sect.* **55**, 331–337.

Fan, C., Li, K., Li, J., Ying, D., Wang, Y. & Jia, J. 2017 Comparative and competitive adsorption of Pb(II) and Cu(II) using tetraethylenepentamine modified chitosan/$CoFe_2O_4$ particles. *Journal of Hazardous Materials* **326**, 211–220.

Freundlich, H. M. F. 1906 Over the adsorption in solution. *Z. Physical Chemistry* **57**, 385–470.

Guo, Y., Deng, J., Zhu, J., Zhou, X. & Bai, R. 2016 Removal of mercury (II) and methylene blue from a wastewater environment with magnetic graphene oxide: adsorption kinetics, isotherms and mechanism. *RSC Adv.* **6** (86), 82523–82536.

Hamza, I. A. A., Martincigh, B. S., Ngila, J. C. & Nyamori, V. O. 2013 Adsorption studies of aqueous Pb(II) onto a sugarcane bagasse/multi-walled carbon nanotube composite. *Physics and Chemistry of the Earth, Parts A/B/C* **66**, 157–166.

Ho, Y. & McKay, G. 1999 Pseudo-second order model for sorption processes. *Process Biochemistry* **34** (5), 451–465.

Karaer, H. & Kaya, İ. 2017 Synthesis, characterization and using at the copper adsorption of chitosan/polyvinyl alcohol magnetic composite. *Journal of Molecular Liquids* **230**, 152–162.

Karthik, R. & Meenakshi, S. 2015 Removal of Pb(II) and Cd(II) ions from aqueous solution using polyaniline grafted chitosan. *Chemical Engineering Journal* **263**, 168–177.

Kefeni, K. K., Mamba, B. B. & Msagati, T. A. M. 2017 Application of spinel ferrite nanoparticles in water and wastewater treatment: a review. *Separation and Purification Technology* **188**, 399–422.

Lagergren, S. 1898 About the theory of so-called adsorption of soluble substances. *Sven. Veten. Handl.* **24**, 1–39.

Langford, J. I. & Wilson, A. J. C. 1978 Scherrer after sixty years: a survey and some new results in the determination of crystallite size. *Journal of Applied Crystallography* **11** (2), 102–113.

Langmuir, I. 1918 The adsorption of gases on plane surfaces of glass, mica and platinum. *Journal of the American Chemical Society* **40** (9), 1361–1403.

Li, X., Lu, H., Zhang, Y. & He, F. 2017 Efficient removal of organic pollutants from aqueous media using newly synthesized polypyrrole/CNTs-$CoFe_2O_4$ magnetic nanocomposites. *Chemical Engineering Journal* **316**, 893–902.

Moradi, A., Najafi Moghadam, P., Hasanzadeh, R. & Sillanpää, M. 2017 Chelating magnetic nanocomposite for the rapid removal of Pb(II) ions from aqueous solutions: characterization, kinetic, isotherm and thermodynamic studies. *RSC Adv.* **7** (1), 433–448.

Nguyen, V. C. & Huynh, T. K. N. 2014 Reusable nanocomposite of $CoFe_2O_4$/chitosan-*graft*-poly(acrylicacid) for removal of Ni(II) from aqueous solution. *Advances in Natural Sciences: Nanoscience and Nanotechnology* **5** (2), 025007.

Olivera, S., Muralidhara, H. B., Venkatesh, K., Guna, V. K., Gopalakrishna, K. & Kumar, K.Y. 2016 Potential applications of cellulose and chitosan nanoparticles/composites in wastewater treatment: a review. *Carbohydrate Polymers* **153**, 600–618.

Panahi, H. A., Mehmandost, N., Moniri, E. & Galaev, I. Y. 2012 Iminodiacetic acid-containing polymer brushes grafted onto silica gel for preconcentration and determination of copper (II) in environmental samples. *Journal of Applied Polymer Science* **126** (2), 480–489.

Reddy, D. H. K. & Lee, S.-M. M. 2013 Application of magnetic chitosan composites for the removal of toxic metal and dyes from aqueous solutions. *Advances in Colloid and Interface Science* **201–202**, 68–93.

Santhosh, C., Kollu, P., Felix, S., Velmurugan, V., Jeong, S. K. & Grace, A. N. 2015 $CoFe_2O_4$ and $NiFe_2O_4$@graphene adsorbents for heavy metal ions – kinetic and thermodynamic analysis. *RSC Adv.* **5** (37), 28965–28972.

Temkin, M. I. & Pyzhev, V. 1940 Kinetics of ammonia synthesis on promoted iron catalyst. *Acta Phys. Chim. USSR* **12**, 327–356.

Tiwari, D. & Mok, S. 2017 Chitosan templated synthesis of mesoporous silica and its application in the treatment of aqueous solutions contaminated with cadmium (II) and lead (II). *Chemical Engineering Journal* **328**, 434–444.

Tshwenya, L. & Arotiba, O. A. 2017 Ethylenediamine functionalized carbon nanoparticles: synthesis, characterization, and evaluation for cadmium removal from water. *RSC Adv.* **7** (54), 34226–34235.

Weber, W. J. & Morris, J. C. 1963 Kinetics of adsorption on carbon from solutions. *J. Sanit. Eng. Div.* **89**, 31–60.

Xiang, B., Ling, D., Lou, H. & Gu, H. 2017 3D hierarchical flower-like nickel ferrite/manganese dioxide toward lead (II) removal from aqueous water. *Journal of Hazardous Materials* **325**, 178–188.

Xiao, Y., Liang, H. & Wang, Z. 2013 $MnFe_2O_4$/chitosan nanocomposites as a recyclable adsorbent for the removal of hexavalent chromium. *Materials Research Bulletin* **48** (10), 3910–3915.

Xu, L., Chen, J., Wen, Y., Li, H., Ma, J. & Fu, D. 2016 Fast and effective removal of cadmium ion from water using chitosan encapsulated magnetic $Fe_3O_4$ nanoparticles. *Desalination and Water Treatment* **57** (18), 8540–8548.

Yadaei, H., Beyki, M. H., Shemirani, F. & Nouroozi, S. 2018 Ferrofluid mediated chitosan@mesoporous carbon nanohybrid for green adsorption/preconcentration of toxic Cd(II): modeling, kinetic and isotherm study. *Reactive and Functional Polymers* **122**, 85–97.

First received 14 August 2018; accepted in revised form 6 December 2018. Available online 14 December 2018